




Rheology of partially solidified hypoeutectic aluminum copper alloys

Lakshmi Ravi Narayan¹  · Rainer J. Hebert¹

Received: 16 February 2022 / Accepted: 13 May 2022

Published online: 24 May 2022

© The Author(s) 2022 

Abstract

This study presents oscillatory and rotational viscosity measurement results on Al-Cu alloys with the goal of achieving effective viscosity data of partially solidified alloys from fully liquid to nearly fully solid state. Rotational viscosity measurements indicate fragmentation of dendrites and a concomitant sudden drop in viscosity of the solid–liquid two-phase mixture upon cooling and increase in solid fraction. This measurement artifact is avoided with oscillatory measurements. The viscosity of partially solid Al-Cu over the hypoeutectic range is nearly composition independent when evaluated as a function of solid fraction. The oscillatory measurements yield a complex viscosity with the real part reflecting the elastic behavior and the imaginary part indicating the viscous part of the viscosity behavior. The measurements of the phase angle in this study reveal that the rheological behavior of the solid phase in the liquid–solid two-phase region resembles that of a liquid more than that of a solid phase.

Highlights

- Oscillatory rheology is shown to be better suited to characterize partially solidified metal alloys than rotational rheology.
- The viscosity of the liquid phase does not change measurably during solidification despite an increase in the solute content.
- The solid phase in the liquid–solid two-phase region behaves rheologically more like a liquid than a solid.

Keywords Rheology · Complex viscosity · Solidification processing

1 Introduction

Alloys solidify over a range of temperatures, starting upon cooling at low to moderate rates at the liquidus temperature of the phase diagram and becoming fully solid at the solidus temperature. During alloy freezing in molds the solid phase nucleates and grows frequently with a dendritic morphology [1]. The dendrites grow with decreasing temperature into the liquid phase, and at a certain temperature within the solidification range begin to contact

each other. Researchers sometimes label this temperature as the coherency point [2, 3]. Below the coherency point the dendrites fuse together to form a network or skeleton upon further cooling, and the solid skeleton then dominates the thermomechanical properties of the solid–liquid mixture. The temperature at which this solid skeleton starts to support tensile stresses is frequently referred to as the rigidity point [4]. Characterizing an alloy in the solidification range has been of interest for understanding manufacturing processes such as casting, welding, semi-solid

✉ Lakshmi Ravi Narayan, lakshmi@uconn.edu | ¹Department of Materials Science and Engineering, University of Connecticut, 97 N. Eagleville Rd., Storrs, CT 06269, USA.



metal forming (thixoforming), and additive manufacturing [4]. In particular, understanding the thermomechanical properties of partially solidified metal alloys is important to the understanding of processing defects such as solidification cracking or hot tearing [5, 6]. Rheological methods can help characterizing the interactions between growing dendrites and the viscosity of inter-dendritic liquid alloy [4]. For example, the propensity of an alloy to crack during solidification processing has been related to the shearing behavior of the partially solidified metal alloy. The shearing of a liquid or semi-solid can be examined with a concentric-cylinder arrangement [6], which has also been used to determine the coherency point [6].

The dendrite coherency point depends on several factors in addition to the alloy composition, including the grain size (also a function of the cooling rate), the directionality of the growth, and the addition of grain refiners [7, 8]. Despite a widespread use of the term “coherency point”, the literature does not completely agree on its definition. Some define it as the point during solidification at which the viscosity rises sharply due to the interaction of the solid crystallites [7]. Others define a rigidity point in addition to the dendrite coherency point [3]. These works define the dendrite coherency point as the point during solidification when isolated crystallites in the liquid matrix interact as they flow past each other but are not large or numerous enough to hinder their flow. The viscosity of this two-phase crystallite-liquid material is still dominated by the liquid. After this point upon further solidification, crystallites flowing in the liquid matrix or dendrites growing from container walls grow large enough to fuse together and form a coherent solid skeleton, and the strength of this two-phase material is dominated by the solid rather than the liquid. This point is known as the rigidity point, and from here on, the viscosity rises even more sharply upon further cooling. Liquid flow is confined to within the inter-dendritic regions. It is beyond this rigidity point that rotational viscosity measurements are no longer reliable, as the solid skeleton breaks and the viscosity is artificially decreased by the formation of globules out of this solid skeleton upon further shearing. The lowering of viscosity due to the breaking of the dendritic structure is exploited in rheocasting or thixoforming [2]. Characterizing this globular structure of metallic alloys by stirring the partially solidified alloy has been done using the concentric cylinder arrangement [9].

Viscosity measurements of solid–liquid mixtures forming a solid skeleton during solidification pose several experimental challenges. While measurements for fully liquid or low solid fractions have relied on viscometers, mixtures containing higher fractions of solid have been characterized using tension, torsion [10, 11] or compression techniques [12]. Viscometers cannot measure torque values that higher solid fractions induce, and tension or

torsional set-ups cannot resolve the low torque values of lower solid fractions. In addition, rotational- or shear measurement techniques tend to break dendritic structures, causing measurement artifacts. The breaking of the dendritic structure can be avoided with rheological measurements using small angle oscillations instead of rotations. Oscillatory rheology is gaining interest in the study of partially solidified metals due to the opportunity to separate the viscous and elastic contribution to the total viscosity; semi-solid metals are visco-elastic or elasto-viscous by nature. Tocci and coworkers used oscillatory measurements to characterize a semi-solid aluminum alloy made into a slurry [13].

This work addresses the rheology of hypoeutectic binary Al-Cu alloys for compositions ranging from 5–30% Cu (by weight). Previous viscosity measurements of Al and Al-Cu focused on the fully liquid state [14]. But with the increasing interest in manufacturing simulations, viscosity data is needed in the solid–liquid two phase region of alloys. This study compares rotational and oscillatory measurements of Al-Cu in the solid–liquid two-phase region. The binary Al-Cu system was selected for this study because it has served over a long time as a model system for solidification studies and for solidification cracking studies. Very recently, for example, the thermodynamics of the fcc phase in the Al-Cu system was re-examined in the undercooled region [15]. The liquid–solid two-phase region plays a key role for solidification cracking and Hu and coworkers examined the crack formation during laser powder bed fusion for Al-Cu [16]. The solidification cracking behavior of Al-Cu alloys was also examined recently under conditions of electro-magnetic stirring of the melt [17, 18]. Oscillatory viscosity measurements have not been widely applied in the field of metallurgy and the current work compares measurement results with those obtained from the more conventional rotational measurements, both of which are described in Sect. 2. The results of both types of experiments are described and compared in Sect. 3. Simulations of manufacturing processes require thermophysical property data over the entire solid–liquid two phase region of alloys and the current work demonstrates how viscosity data can be obtained for solid fractions approaching the completely solid state.

2 Materials and methods

Alloys with nominally 5, 10, 20 and 30 wt % copper in aluminum were synthesized using 99.999% metals basis (Sigma Aldrich) in a vacuum arc furnace (Materials Research Furnaces ABJ-900–3). The arc-melted pieces were ultrasonically cleaned in ethanol prior to testing.

A Searle-type [19] concentric-cylinder rheometer (Anton Paar FRS1800) was used in this work. A schematic of the experimental set-up is shown in Fig. 1. A fixed outer cylinder (30 mm diameter) made from alumina contains the sample, into which the smaller inner alumina cylinder (15 mm diameter, 20 mm length, profiled surface) is suspended by means of an alumina spindle (5 mm diameter). This spindle allows for the controlled rotation and oscillation of the inner cylinder, and for the torque experienced by it to be measured. The cylinders are housed in a tube furnace capable of operating at up to 1800 °C. A thermocouple placed at the bottom of the outer cylinder was used to monitor the temperature of the test. The measured test temperature is within ± 3 °C of the set point. During the test, a gas mixture of 2% hydrogen in argon streamed through the length of the furnace to reduce oxidation. The calibration of the rheometer was verified using a glass standard (NIST 717a), and the viscosity was found to be within 5% of the specified value.

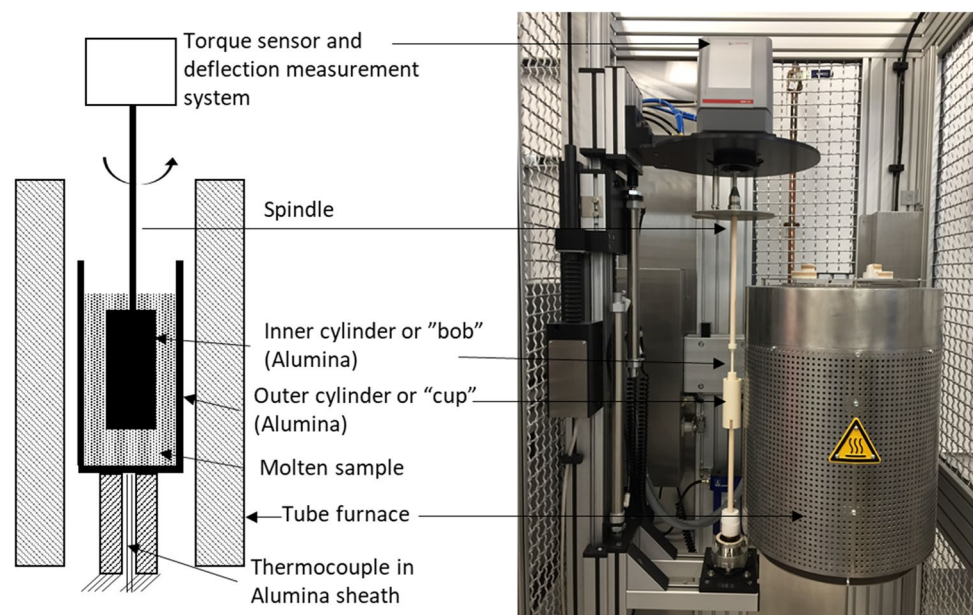
Before each set of measurements, the furnace was heated up to 720 °C to completely melt the charge, cooled to the test temperature and held until equilibrium, and then the following set of measurements were made: sinusoidal oscillations of 1 mrad amplitude and 1 Hz frequency, sinusoidal oscillations of 10 mrad amplitude and 1 Hz frequency, rotations at a shear rate of 1 s^{-1} , and rotations at a shear rate of 10 s^{-1} . The sample was then re-heated to 720 °C before cooling to the next lower test temperature. Ten repeating measurements of each were made, and the average was reported. Each set of measurements for a temperature is independent of the measurements made at the other temperatures by completely re-melting the sample before the next lower test temperature. Most

importantly, after reaching a test temperature, the sample was not sheared to break dendrites into globules prior to the viscosity measurement. Instead, the quiescent melt was kept until equilibrium was established before the viscosity measurements.

During sinusoidal oscillatory displacement of the inner cylinder, the torque follows a sinusoidal change with time, but in general with a phase shift δ , from which the complex viscosity is determined [20]. The real component of the torque, which is in phase with the displacement is the elastic component of the complex viscosity, and the imaginary component which is out of phase with the displacement is the viscous component. The angle between the complex viscosity vector and its elastic component is the phase shift or loss angle δ ; For a fully elastic solid, the response variable, for example, the torque follows the control variable, displacement, without any phase shift. For ideally viscous materials, the phase shift or loss angle is 90° [20].

Fractions of solid curves and compositions of the liquid phase were determined using a computational thermodynamics software, Pandat Computherm, using the equilibrium model and from differential scanning calorimetry (DSC) measurements using a Netzsch Pegasus F1 404 heat-flux calorimeter. The DSC measurements were performed in cooling mode from a starting temperature of 720 °C and at a cooling rate of 10 K/min. The sample temperature of the calorimeter was calibrated using standard methods of melting points of high-purity metals (In, Sn, Zn, Al, Au). The typical sample mass was about 5 mg, Pt/Rh crucibles with Al_2O_3 liners were used for the measurements. The sample space in the DSC was evacuated prior to the measurements to a vacuum of about 2×10^{-2} Torr and

Fig. 1 Schematic of the concentric cylinder rheometer used in this work



then backfilled with 99.999% pure argon gas; a 100 ml/min constant flow of argon gas was used during the measurements. Nominal compositions of the alloys were used as input.

A sample was prepared for microstructural analysis after testing by sectioning the solidified material around the inner cylinder and polishing using standard metallographic techniques. Optical micrographs were obtained using a Zeiss Axiomager A2.

3 Results

Figure 2 shows the results of continuous cooling DSC measurements of the four alloy compositions. The onset of solidification and formation of primary aluminum occurs with an abrupt transition in the signal and exothermic peak. A second exothermic peak then occurs at lower temperatures that represents the formation of the eutectic phase. Liquidus and eutectic temperatures are summarized for the four alloys in Table 1. The DSC measurements shown in Fig. 2 are referenced in the following in the context of the viscosity measurements. Results of rotational viscosity measurements are shown in Fig. 3 for constant shear rates of 1 and 10 s⁻¹. The 5 wt % alloy starts to solidify at 647 °C according to the thermodynamic calculations and at 642 °C according to the DSC measurements.

The solid fraction is shown in Fig. 4 as a function of temperature, obtained from thermodynamic calculations. For the 5 wt % alloy, the viscosity increases rapidly at about 595 °C at which the solid fraction is about 95%. The viscosity then drops and shows a lower value at the lowest recorded temperature of 560 °C than at 595 °C. The lower

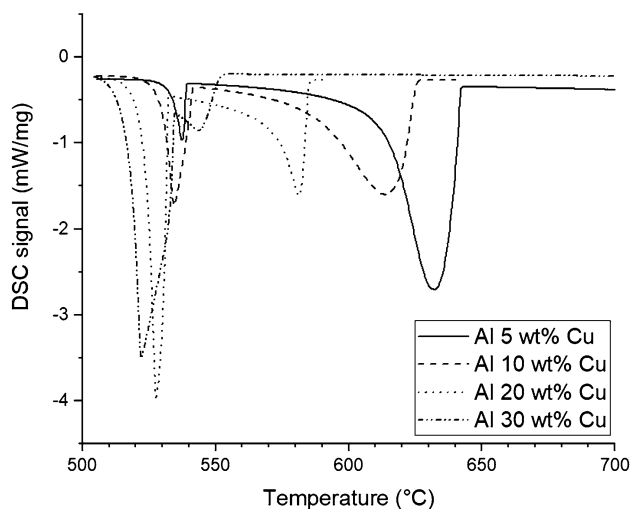


Fig. 2 Continuous cooling DSC curves for Al-5, 10, 20, and 30 wt % Cu alloys

Table 1 Thermodynamic and experimental data for liquidus and eutectic temperatures and their differences

		T_l (°C)	T_e (°C)	$T_l - T_e$ (°C)
Al 5 wt % Cu	Lever	647	548	99
	Scheil	647	–	–
	Experiment	642	539	97
Al 10 wt % Cu	Lever	634	548	86
	Scheil	634	548	86
	Experiment	627	542	85
Al 20 wt % Cu	Lever	604	548	56
	Scheil	604	548	56
	Experiment	586	532	54
Al 30 wt % Cu	Lever	564	548	16
	Scheil	564	548	16
	Experiment	554	535	19

temperature limit of 560 °C for the rotational measurements was chosen to protect the equipment from too high of a torque of the freezing alloy liquid. The liquid portion of the hypoeutectic Al-Cu compositions forms a eutectic under equilibrium conditions at 548 °C while the DSC measurements indicate a eutectic temperature of 539 °C. The temperature range from the onset of solidification of the 5 wt % alloy to the eutectic temperature is 98 °C according to the thermodynamic calculation and 97 °C in the DSC measurement.

The solid fraction and the viscosity as a function of temperature are combined in Fig. 5 to yield the viscosity directly as a function of the fraction solid. For the 5 wt % alloy it is seen that the viscosity indeed decreases at the highest solid fractions. The viscosity values reveal an almost order of magnitude difference between the two applied shear rates with the 10 s⁻¹ shear rate inducing lower viscosity values than the 1 s⁻¹ shear rate. The 10 wt % Al-Cu alloy shows a behavior similar to the 5 wt % alloy although the increase in viscosity at 595 °C is not as pronounced as for the 5 wt % alloy because the solid fraction is less at that temperature than for the 5 wt % alloy. The comparison between the viscosity as a fraction solid for the 5 wt % and the 10 wt % alloys shows that between 60 and 70% solid the 10 wt % alloy has a higher viscosity than the 5 wt % alloy, but this difference decreases with increasing shear rate. For the 80 to 90% solid range, the viscosity values of the 5 and 10 wt % alloys cannot be directly compared because measurements occurred at slightly different solid fractions, but a coarse fit of the data for the two alloys suggests that the viscosity values in that solid fraction range could nearly coincide for the two compositions. The maximum measurable solid fraction of primary aluminum is capped for the 10 wt % alloy at about 86% when the remaining liquid forms a eutectic

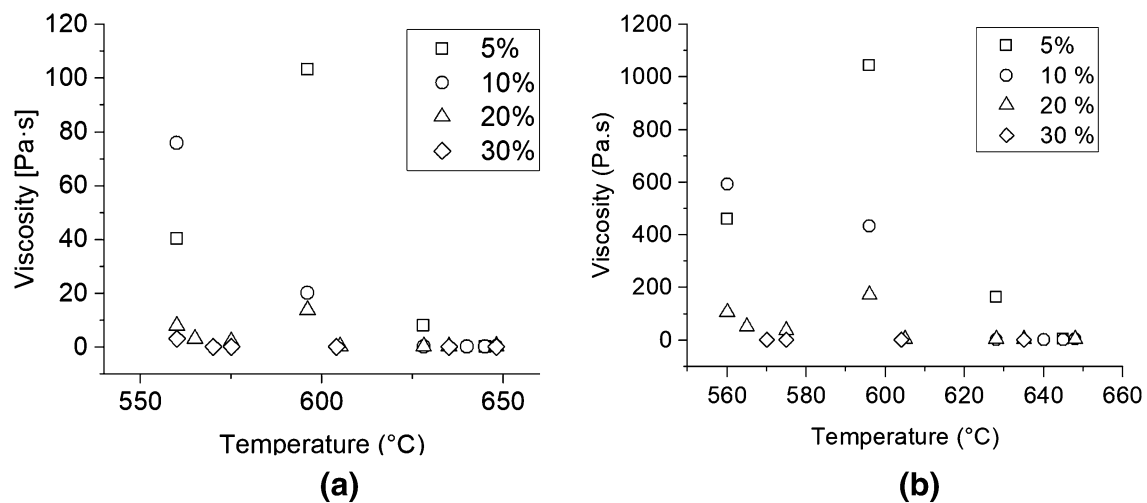


Fig. 3 Rotational viscosity measurements at a shear rate of **a** 10 s^{-1} and **b** 1 s^{-1} for 5, 10, 20 and 30% Cu (by weight) in Al

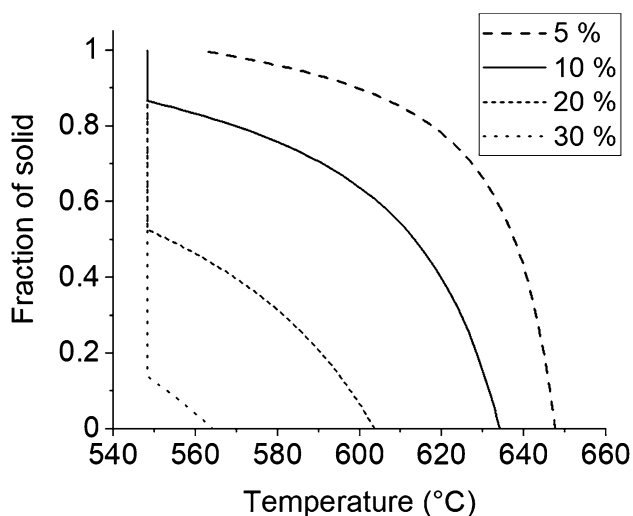


Fig. 4 Fraction of solid vs. temperature for the four different compositions of the Al-Cu alloys used in this work. The plots were generated using CompuTherm thermodynamic software using the equilibrium/Lever model

at the eutectic temperature. The temperature range from the onset of solidification of the 10 wt % alloy to the eutectic temperature is $86 \text{ }^\circ\text{C}$ according to the thermodynamic calculation and $85 \text{ }^\circ\text{C}$ in the DSC measurement. The 20 wt % alloy follows the same trend with an increase in viscosity in the solid-liquid region at about $595 \text{ }^\circ\text{C}$ that is less pronounced than for the 10 wt % alloy and a slight decrease toward lower temperatures before the viscosity then slightly increases again. Because of the higher alloy content, the increase in viscosity at $595 \text{ }^\circ\text{C}$ occurs at a lower solid fraction of about 12 wt % as seen in Fig. 5. The temperature range from the onset of solidification of the 20

wt % alloy to the eutectic temperature is $56 \text{ }^\circ\text{C}$ according to the thermodynamic calculation and $54 \text{ }^\circ\text{C}$ in the DSC measurement. The highest alloy composition of this study, 30 wt %, starts to solidify at about $564 \text{ }^\circ\text{C}$ and the temperature range from the onset of solidification of the 30 wt % alloy to the eutectic temperature is $16 \text{ }^\circ\text{C}$ according to the thermodynamic calculation and $19 \text{ }^\circ\text{C}$ in the DSC measurement.

The thermodynamic calculations demonstrate that the temperature difference between the onset of solidification and the eutectic temperature upon cooling depend sensitively on the alloy composition and the experimentally measured temperature difference closely matches the thermodynamic data as Table 1 demonstrates. The temperature range between liquidus and eutectic temperatures can be used to estimate how much the actual alloy compositions deviated from the nominal compositions. The temperature range, $\Delta T = T_l - T_e$, can be described as a function of the alloy composition, x , in weight percent copper with a quadratic polynomial function

$$\Delta T(x) = 108.7 - 1.78 * x - 4.3 * 10^{-2} * x^2 \quad (1)$$

This temperature range, which is calculated using the Lever rule and CompuTherm Pandat™ thermodynamic software is shown in Fig. 6 as a function of Cu content.

The difference between experimental and thermodynamic model ΔT can then be used to estimate the corresponding difference in alloy content. For example, this difference is $2 \text{ }^\circ\text{C}$ for the 5 wt % composition. For the slope of the $\Delta T(x)$ curve at 5 wt % copper, a difference in temperature of $2 \text{ }^\circ\text{C}$ corresponds to a variation in composition of about 0.8 wt %, i.e., the actual composition of the alloy can be estimated to be 5.8 wt %. The same approach

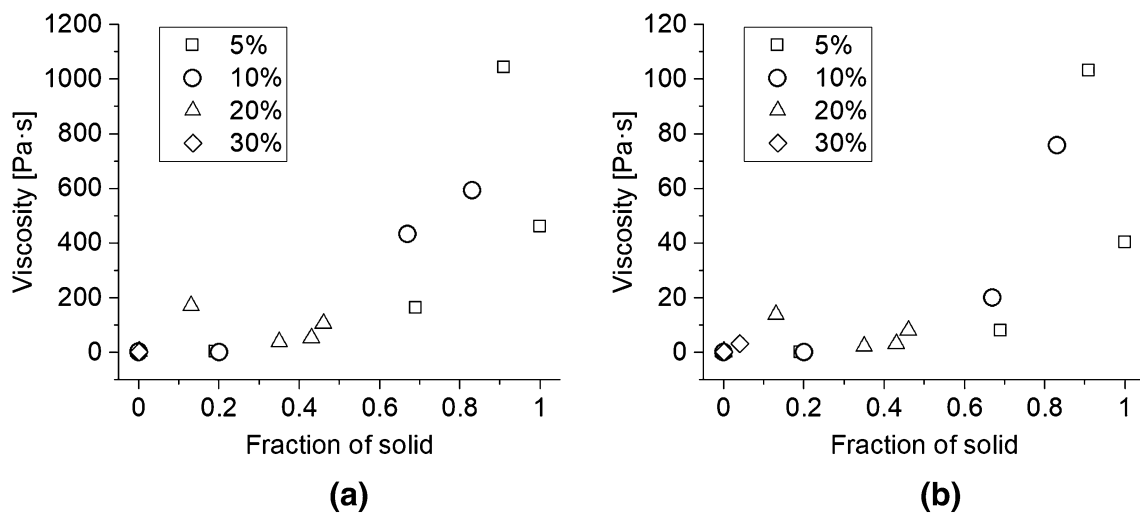


Fig. 5 Rotational viscosity measurements plotted against fraction of solid at a shear rate of **a** 1 s⁻¹ and **b** 10 s⁻¹ for 5, 10, 20 and 30% Cu (by weight) in Al

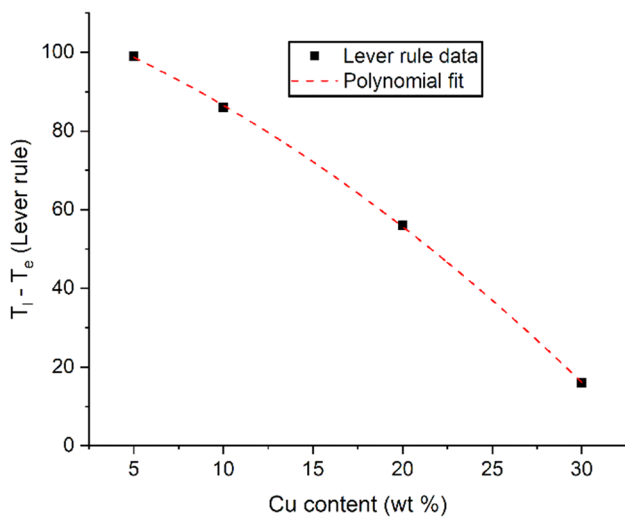


Fig. 6 Plot of temperature difference between liquidus and eutectic temperature based on the Lever rule for Al-Cu binary alloys as a function of the Cu content (in wt %)

yields an actual composition of about 10.4 wt % instead of the nominal 10, 20.6 wt % instead of 20, and 29.4 instead of 30%. Differences in the rate of evaporation between aluminum and copper during arc-melting can cause the observed increase in the actual composition over the nominal composition if aluminum evaporates more than copper. For the 30 wt % alloy, the reason for the observed difference between nominal and actual composition cannot be unambiguously determined.

Oscillatory viscosity measurement results are plotted in Fig. 7 along with the corresponding fraction solid curves for each alloy for an amplitude of 1 mrad and a frequency

of 1 Hz. Oscillatory viscosity for the Al 5 wt % Cu alloy in Fig. 7a shows a steady rise in viscosity with increasing fraction of solid, the steepest rise being between 20 and 60% fraction of solid. This is also the case for the 10 wt % Cu alloy in Fig. 7b. For the 20 wt % (Fig. 6c) and 30 wt % Cu (Fig. 7d) alloys, the solidification range is small and the distinct rise in viscosity appears to occur at the onset of solidification. The drop in the viscosity at high fractions of solid that was seen in the rotational viscosity measurements are not seen in the oscillatory measurements. Moreover, the viscosity values span about four to five orders of magnitude as the liquid alloy completely solidifies for the oscillatory measurements but only two to three orders of magnitude for the rotational measurements. For all four alloys and over the solidification range, the real part of the complex viscosity is less than the imaginary part. The complex viscosity largely coincides with the imaginary part. This behavior is reflected also in the loss angle, δ , shown in Fig. 8. Below the temperature of the onset of solidification, the loss angle decreases from above 85° to between 60 and 70° for all alloys. A loss angle of close to 90° indicates a purely viscous behavior, i.e., a near zero elastic component. Since the real part of the viscosity reflects the elastic contribution, the complex viscosity in the liquid state is approximately identical with the imaginary part. Figure 9 shows that the loss angle is a sensitive indicator of the existence of a liquid phase in the solid-liquid two phase region: the loss angle drops rapidly with the onset of solidification from the near 90° value to 60–70°. Over the solidification range then the loss angle remains relatively constant. Values of the loss angle of over 45° are typically interpreted as being indicative of a liquid rather than a solid.

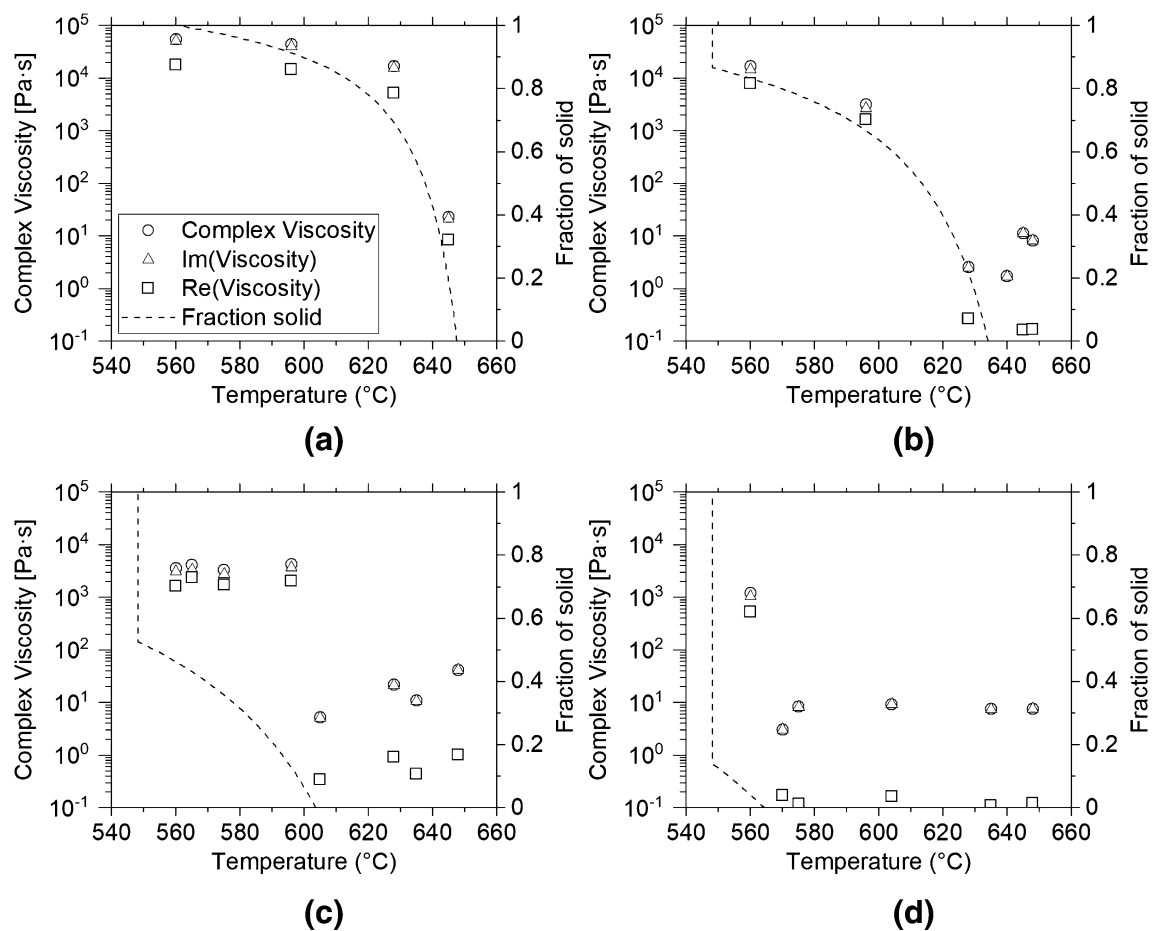


Fig. 7 Oscillatory measurements at an amplitude of 1 mrad and a frequency of 1 Hz- **a** 5%, **b** 10%, **c** 20% and **d** 30% (by weight) Cu

Oscillatory measurements were also performed at an amplitude of 10 mrad with the same frequency of 1 Hz. These measurement results are shown in Fig. 9. The same trend is seen in the behavior of the 5 wt % alloy as for the oscillations at 1 mrad: the viscosity increases sharply between a fraction of solid of 20 and 60%. For the 10 wt % Cu alloy, the viscosity also increases sharply in the same fraction solid range. The 20 and 30 wt % alloys which have a short solidification range show this increase when the solidification begins. Much like for the rotational measurements, the viscosity values decrease by about an order of magnitude with the increase in this case in the amplitude of oscillation by one order of magnitude. The shear strain rate therefore increased, since the frequency of oscillations was kept at 1 Hz. The loss angles for these measurements, which are shown in Fig. 10, demonstrate a drop from above 85° in the fully liquid region to between 50 and 60° at the onset of solidification. The loss angle therefore decreased slightly in the solid–liquid two phase region with the increase in the oscillation amplitude.

During solidification of the hypoeutectic Al–Cu alloy the liquid becomes enriched in solute due to microsegregation. For any nominal composition of a hypoeutectic alloy, the liquid composition changes with temperature in the solid–liquid two phase region. From the binary phase diagram, the equilibrium composition can be inferred of the liquid at any temperature. For a nominal 5 wt % alloy the liquid composition was thus determined for four different temperatures in the solid–liquid two phase region and for each of these liquid compositions a sample was prepared that had the same nominal composition as the liquid composition of the 5 wt % alloy. Upon melting in the furnace rheometer, it was therefore possible to assess the viscosity of the liquid portion alone of the nominally 5 wt % alloy, without the influence of the solid skeleton. In Fig. 11, the complex viscosity of the nominally 5% alloy is compared with the viscosity of the four alloys that had the same composition as the liquid fraction of the nominally 5 wt% alloy at those temperatures. Figure 11 demonstrates that the viscosity of the liquid alloys and hence of the liquid phase

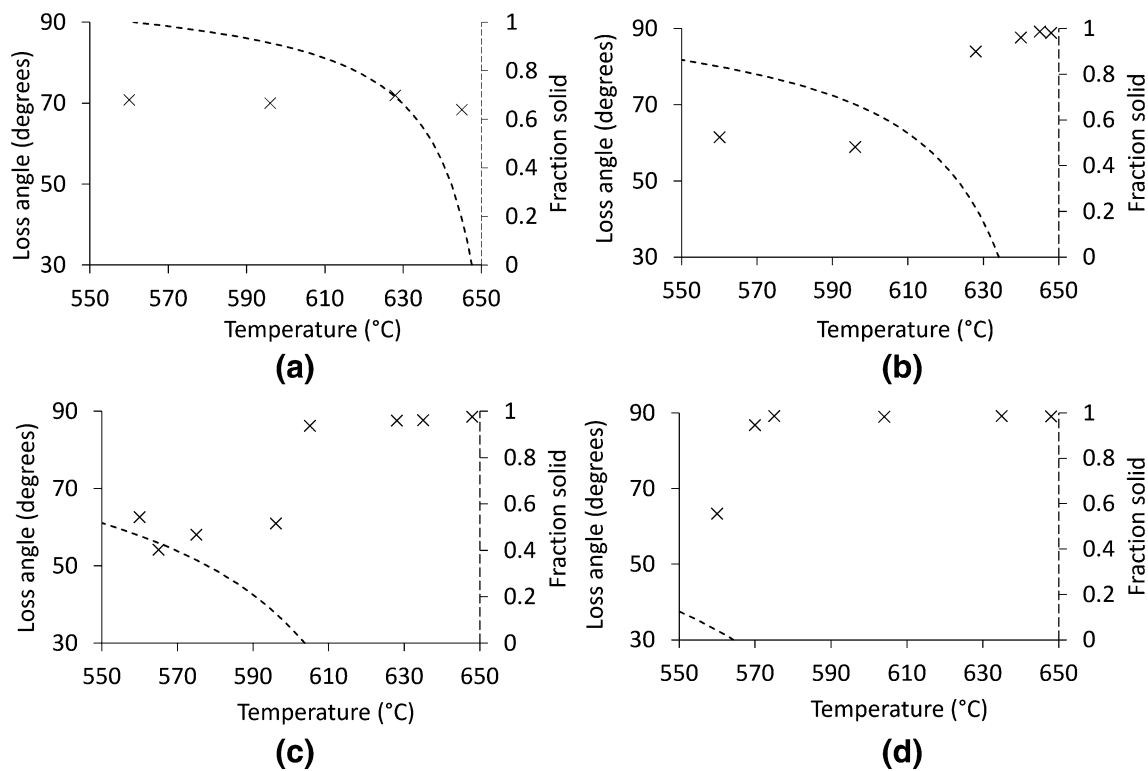


Fig. 8 Loss angle δ for the oscillatory measurements in Fig. 5- **a** 5%, **b** 10%, **c** 20% and **d** 30% (by weight) Cu

of the nominally 5 wt % alloy in the solid–liquid two phase region is largely invariant with composition.

The optical micrographs in Fig. 12 show the solidified microstructure of the 5 wt % sample around the inner cylinder after furnace cool down, which took approximately 10 h. The micrographs were taken from three different locations along the length (height) of the inner cylinder. The normal to the image plane points along the tangential direction of the inner cylinder and the coordinate system orientation relative to the inner cylinder geometry is shown in Fig. 12a. The micrographs indicate a directionality of the primary dendrites, which appear to grow slightly upward at an angle of approximately 25° to the cylinder axis, which is indicated in Fig. 12, image 2, with a dashed orange line. The direction of the primary dendrites is indicated with a dashed yellow line. The angle between these two directions is about 25° . The micrographs shown in Fig. 12 demonstrate that the crystalline phase develops with a dendritic growth morphology and not with an equiaxed one. The latter growth morphology is induced intentionally for thixoforming applications, but in the current work the viscosity was measured without pre-shearing. The crystalline phase therefore developed as it would in a casting before the shearing of the cylinder started. The primary dendrite growth direction aligns roughly with the thermal gradient and primary growth directions of

fcc metals are typically aligned with the $\langle 100 \rangle$ crystallographic direction. In the current work the angle that the dendrites form with respect to the cylinder wall indicate a thermal gradient in the cylinder gap that deviates from a simple radial orientation. The deviation could be caused by the boundary conditions that the melt experiences. The alloy melt is contained in an alumina cylinder cup and is exposed on top to the furnace. A vertical upward flow of the argon–hydrogen mixture in the furnace core could cause sufficient convection at the alloy surface to induce the temperature gradient that causes the observed orientation of the primary dendrites.

4 Discussion

A common notion is that pure metals in their liquid state reveal a Newtonian flow behavior although recently reports emerged that indicate non-Newtonian behavior for some metals [21]. If a material displays a Newtonian flow behavior the viscosity does not depend on the shear rate and hence the shear stress scales linearly with the shear strain [20]. While the question if some liquid metals behave in a non-Newtonian manner requires further study, it is less disputed that liquid metals containing inclusions and oxides do show a shear thinning behavior [22, 23]. In

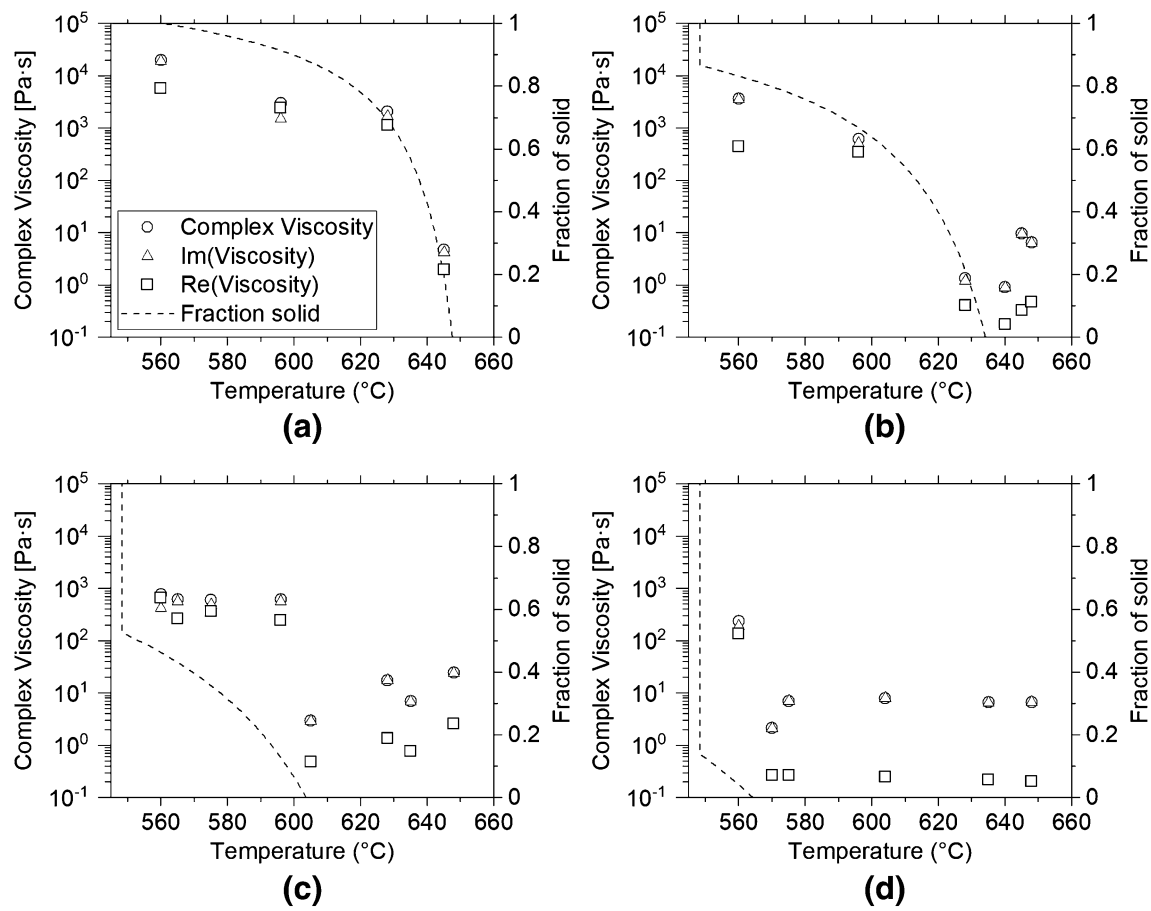


Fig. 9 Oscillatory measurements at an amplitude of 10 mrad and a frequency of 1 Hz- **a** 5%, **b** 10%, **c** 20% and **d** 30% (by weight) Cu

addition to the presence of oxides and inclusions inherent to the alloy melt, dendrites or solid phase particles growing with other morphologies represent a dispersed phase in the liquid matrix phase that induces a non-Newtonian behavior. A comparison of the rotational viscosity measurements in Fig. 3a and b shows a decrease in the viscosity by about one order of magnitude with an increase in the shear rate by one order of magnitude. This shear thinning effect, which is common for practical metal alloys is comparable with the results obtained for an A356 aluminum alloy over a temperature range in the liquid–solid two phase region and for shear rates of 1 and 10 s^{-1} [24]. The apparent viscosity, η , of the solid–liquid two phase region follows the shear rate, $\dot{\gamma}$, with a power-law model [25]:

$$\eta = K \cdot \dot{\gamma}^n \quad (2)$$

The viscosity has the unit of Pa*s, the shear rate has the unit of 1/s. In the current work the two shear rates and the corresponding viscosity values yield a value of the exponent in Eq. (2), n , of approximately -0.9 to -1 over the temperature range measured and the different

alloy compositions. By comparison, for the same shear rates and an A356 alloy, Ma and coworkers found values of the exponent of about -1.1 [24]. The observed shear rate dependence of the effective viscosity for the partially solidified melt is significant from an application viewpoint. In most applications the liquid solidifies under flow conditions that induce shear at least near surfaces or interfaces. Higher filling rates of molds, for example, during die casting promote lower viscosities of the semi-solid alloy, which generally improves the complete filling of the die [26, 27].

The coherency and rigidity points or temperatures should be reflected in the rheological behavior of the solid–liquid two phase alloy. At the coherency point the dendrites start to touch according to some definitions, but it is not until the rigidity point that the solid phase can sustain tensile stresses. The notion of a rigidity point and interlocking dendrite arms is conceptually appealing, but it is limited to the localized or microscopic aspect of dendrite arm interactions. It does not consider the shape at which the crystallites and dendrites grow in the gap of the rotational measurement devices. A globular morphology of dendrites develops during intense shearing and is

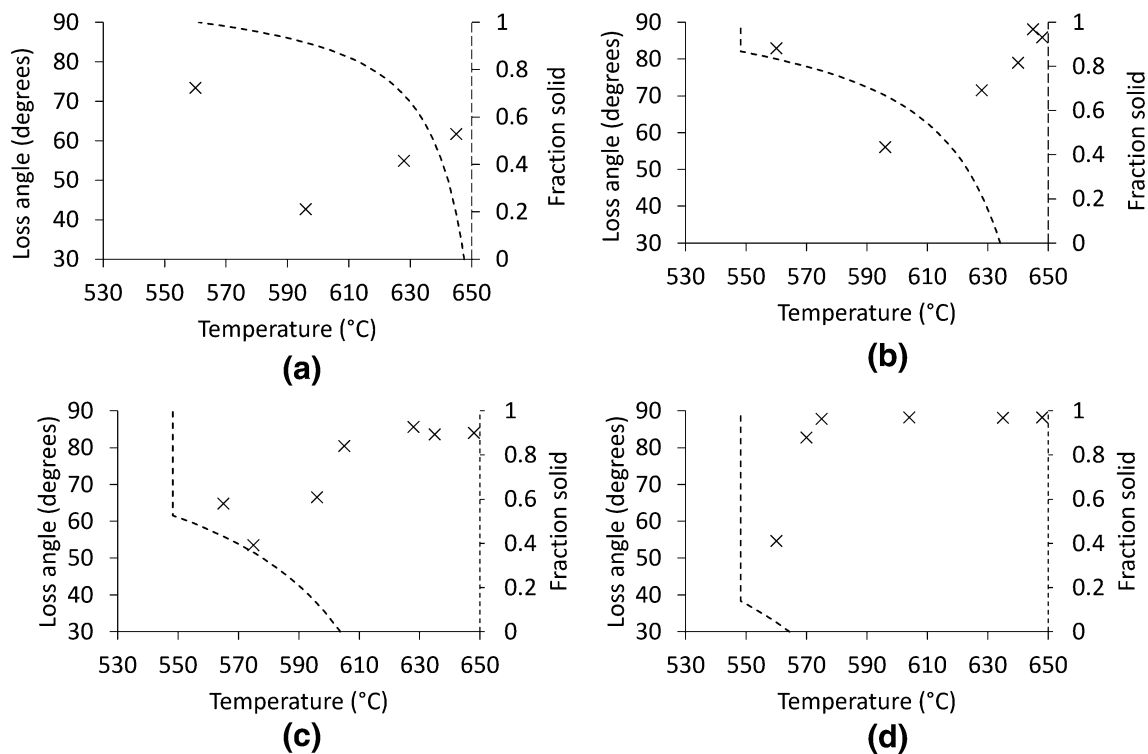


Fig. 10 Loss angle δ for the oscillatory measurements in Fig. 7- **a** 5%, **b** 10%, **c** 20% and **d** 30% (by weight) Cu

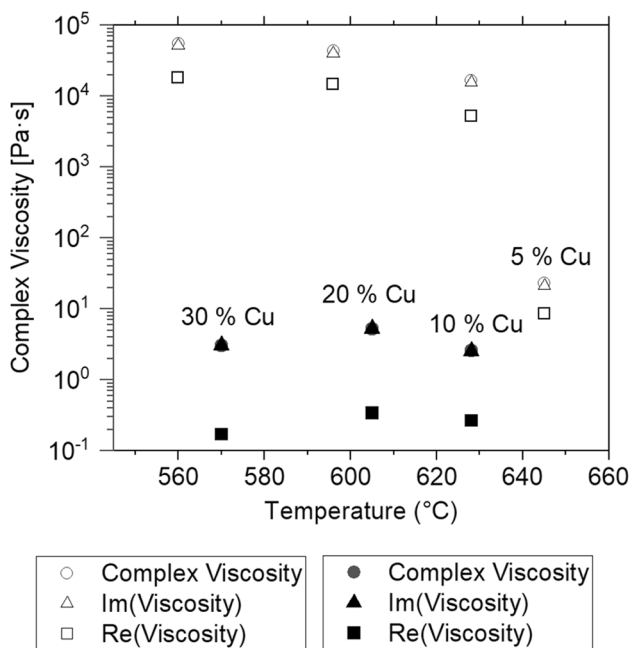


Fig. 11 Oscillatory measurements of the compositions of the liquid fractions of the 5 wt % alloy. The hollow markers are the measurements of the partially solidified 5 wt % alloy, and the solid markers are the measurements of nominally 10, 20 and 30 wt. % alloys, which are also the compositions of the liquid portion of the partially solidified 5 wt. % alloy at those temperatures

the basis for thixoforming applications [2]. The intense shearing to induce globules and viscosity measurements of solid-liquid two phase mixtures with solid globules are important for semi-solid processing such as thixoforming, but they would not reflect the solid-liquid mixture developing in other manufacturing processes. In welding, casting, or additive manufacturing elongated dendrites or cells are more commonly found that are aligned parallel and in directions that vary with the solidification velocity between the direction of thermal gradients in the melt-pool and the crystallographic orientations of the dendrites [28]. The temperature-shear profile used in the current work was chosen to yield results that are better suited for viscosity assessments of welding, casting, or additive manufacturing where elongated rather than globular dendrites or cells develop. The optical micrographs shown in Fig. 12 indeed demonstrate that the liquid alloy in the gap of the rheometer solidified with elongated rather than globular dendrites. The rotational measurement results shown in Figs. 3 and 5 reveal an increase in viscosity during cooling then a decrease that only increases again as the eutectic starts to form. The viscosity measurements in this work were performed after the liquid-solid two-phase mixture was kept in the rheometer cup at temperature for some time and without shearing. The observed viscosity increase and drop upon cooling occurs if parts of dendrites broke off as a result of the shearing. The oscillatory

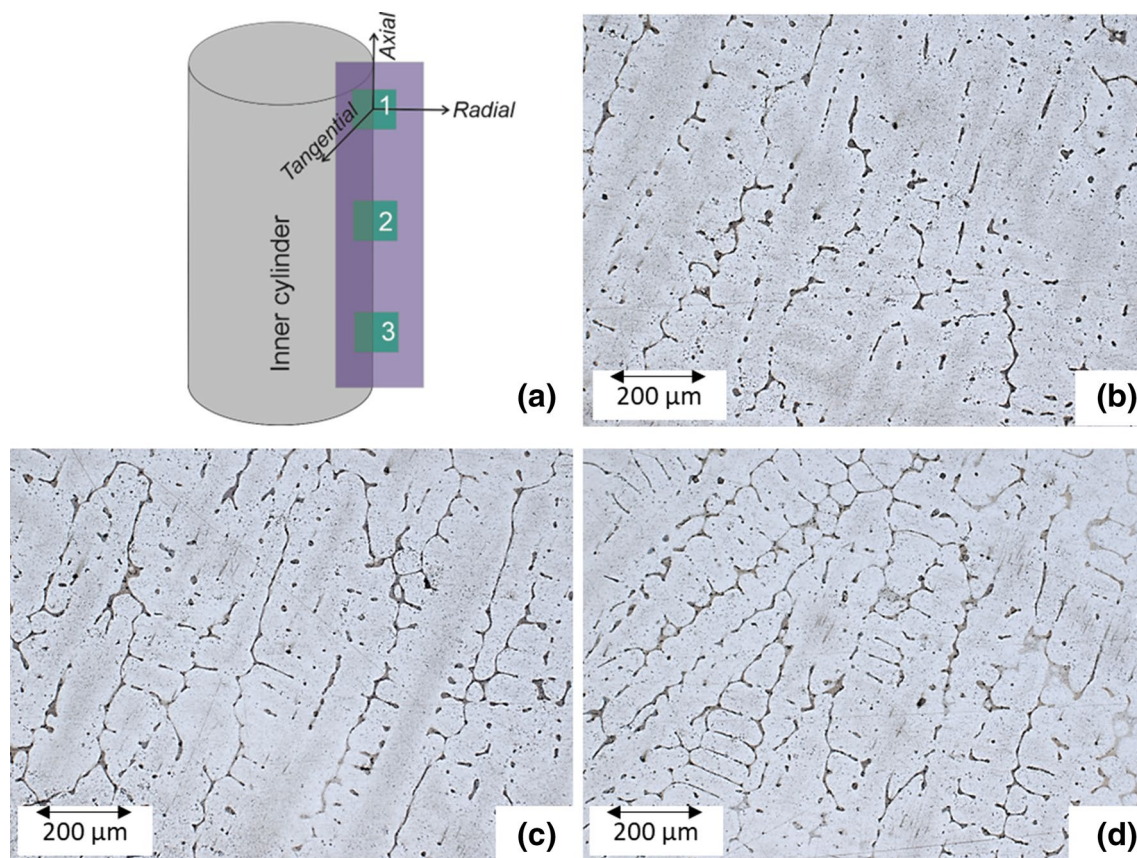


Fig. 12 Optical micrograph of the longitudinal cross-section of the solidified Al 5 wt % Cu alloy at the sides of the inner cylinder. Micrograph (b) shows the solidified alloy near the inner cylinder surface toward the top of the cylinder (location '1' in (a)), micrograph

(c) shows the sample near the half height of the cylinder, and (d) shows the micrograph near the bottom of the cylinder. All micrographs are oriented with the normal to the image plane pointing in the tangential direction

measurements, by contrast, reveal a continuous increase in viscosity with rising solid fraction. The amplitudes chosen in the current work of 1 mrad and 10 mrad are likely too small to cause dendrite tips to break and instead probe the dendrite structure without the measurement interfering and fragmenting the structure. The steep rise in the viscosity that occurs between fraction solid 0.2 and 0.6 has been identified in previous rheological studies of metal alloys as the region between the dendrite coherency point and the rigidity point [5]. The oscillatory measurements yield a monotonic increase in the viscosity of the partially solidified melt and are therefore better suited than the rotational measurements to capture the viscosity of the solid-liquid two phase mixture over the solidification range.

A striking feature of the oscillatory measurements is the behavior of the phase shift or loss angle for the 1 mrad amplitude measurements, which show a near constant value of 85–90° in the liquid and slightly solidified range to then drop sharply to about 65–70° upon further solidification. The phase shift, δ , indicates the lag of the

response variable, torque in this work, behind the control variable, the displacement angle in this work. Figure 13 shows the relation between complex viscosity, real and

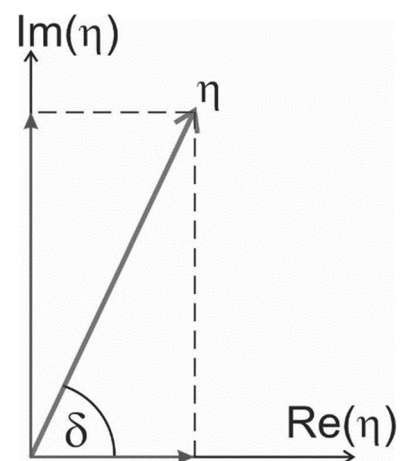


Fig. 13 Geometrical interpretation of phase shift or loss angle, δ , and real and imaginary part of complex viscosity, η

imaginary part, and the phase shift angle. The latter is measured between the real part of the complex viscosity and the complex viscosity vector. At temperatures above or just below the liquidus temperature a viscous behavior is expected, since the alloy is liquid or mostly liquid; a viscous behavior is indeed reflected in the phase shift that would be 90° for an ideally viscous material. At high solid fractions and approaching the eutectic transformation, the phase shift remains above 45° for the 1 mrad amplitude measurements. A phase shift between 0 and 45° indicates a solid behavior while angles above 45° generally indicate a liquid-type behavior [20]. The current measurements therefore suggest that even at a significant solid fraction the liquid–solid two-phase mixture behaves more like a liquid than a solid. For the 10 mrad amplitude measurements, the change in the phase shift is less pronounced with solidification, but except for one data point, the phase shift remains above 45° . Indeed, solid metals at high temperatures behave visco-elastically. For this reason, the viscous and elastic components cannot be separated into liquid and solid contributions.

The viscosity analysis in the current work assumes a laminar flow in the rheometer gap without secondary flows. Above a threshold shear rate, measurements could be affected by turbulence in the rheometer gap. The Taylor instability criterion predicts at which values of the viscosity turbulence is expected for the rheometer geometry used for this work. The Taylor instability condition can be calculated from Eq. (3) [29]:

$$\frac{\omega \cdot r_1 \cdot (r_2 - r_1)}{\left(\frac{\mu}{\rho}\right)} \cdot \sqrt{\frac{(1 - \beta)}{\beta}} > 41.3 \quad (3)$$

R_1 represents the radius of the cylinder, r_2 the radius of the outer cup; μ is the viscosity, ρ is the density, β equals the ratio r_1/r_2 , and ω is the angular frequency $2\pi f$ with f as the frequency. With the diameters of 15 mm and 30 mm, respectively, for the cylinder and the stationary cup, a density of 2.7 g/cm^3 of aluminum, and a viscosity of $4 \text{ mPa}\cdot\text{s}$ for pure liquid aluminum, the critical frequency above which secondary flow would commence is 749 s^{-1} . This critical frequency decreases to 30 s^{-1} when the viscosity increases to $0.1 \text{ Pa}\cdot\text{s}$. The oscillatory measurements were based on shear angles of 1 mrad and 10 mrad at 1 s^{-1} . The 1 mrad oscillation covers $2 \cdot 0.057^\circ \text{ s}^{-1}$. At this angular velocity a full rotation of the measurement cylinder would correspond to a frequency of $3.16 \cdot 10^{-4} \text{ s}^{-1}$. Since the Al-Cu alloys in the liquid–solid two-phase region reveal non-Newtonian behavior, the considerably lower shear rate of the oscillatory mode compared to the rotational mode imparts higher viscosity values. The viscosity values measured with the oscillatory mode approach $10^5 \text{ Pa}\cdot\text{s}$ for

the 5 wt % alloy, for example, while the rotational measurements varied with increasing solidification because of the likely dendrite fragmentation, but was generally in the $400\text{--}1000 \text{ Pa}\cdot\text{s}$ range (Fig. 3). The difference is therefore approximately three orders of magnitude while the shear rate difference is about 3.8 orders of magnitude. The exponent of about -0.9 to -1.0 in Eq. (1) that reflects the viscosity changes for the two rotational shear rates therefore does not apply exactly at the much lower shear rates found for the oscillatory measurements. A non-Newtonian flow behavior is usually explained based on short-range structural changes in a liquid [30]. If the oscillatory measurement approach probes the essentially undisturbed partially solidified alloy melt and does not affect the nature of the liquid as the rotational measurement appears to do, then one might expect less of a non-Newtonian behavior compared to the rotational measurement approach. A comparison between the data in Figs. 7 and 9 shows that the viscosity still changes upon an increase from 1 mrad to a 10 mrad amplitude at equal shear rate and therefore an increased angular velocity of the measurement cylinder. But the viscosity change for the different measurement temperatures is less than one order of magnitude for the real and imaginary parts and therefore smaller than the change for the rotational measurements. The viscosity measurements of the partially solidified melt probe solid and liquid phase and even with small oscillations it is likely that the solid phase responds with changes in defects and that these changes would depend on the amplitude and rate of the oscillations, which would contribute to a non-Newtonian behavior.

The oscillatory measurement results show that the real part of the complex viscosity is lower than the imaginary part, with the imaginary part very closely matching the complex viscosity. These results are consistent with the phase shift angle of more than 45° . Figure 13 shows the imaginary and real part of the complex viscosity for a phase shift angle δ of 60° . The real part is less than the imaginary part and this difference increases as the phase shift angle increases. The difference between real and imaginary components of the viscosity are the largest in the liquid state when the phase shift is close to 90° . The current work suggests that even in the fully liquid condition the real part is non-zero. Further work is necessary to understand the origin of an elastic contribution to liquid alloy viscosity. Early work by Jones and Bartlett demonstrated a “change point” in liquid binary aluminum alloys at 765 to $770 \text{ }^\circ\text{C}$ [31]. Above the change point the viscosity remained temperature independent, but below it showed a slight increase with decreasing temperature and explanations revolved around a potential short-range ordering of the alloy melt as it approached the liquidus temperature. But other factors could as well contribute

to an elastic component, for example, the presence of a thin oxide skin on the liquid alloy surface. When the alloy melt enters the partially solidified temperature range the elastic portion of the complex viscosity could be attributed mainly to the solid phase and the imaginary part to the liquid phase. However, Fig. 11 sheds a different light on this presumption. The viscosity of interdendritic liquid was measured with separate measurements of fully liquid samples that had the same composition as the interdendritic liquid of the Al-Cu alloys in this study. Real and imaginary parts of the viscosity of the interdendritic liquid are orders of magnitude smaller than those observed for the partially solidified alloys: The separate measurements of liquid of the same composition as the liquid portion for the Al-Cu alloys used in this study show viscosity values of 30–40 Pa*s, far below the $4\text{--}5 \times 10^4$ Pa*s of the liquid–solid two-phase mixtures. The imaginary viscosity data of the partially solidified alloy therefore represents predominantly the solid phase, since the contribution of the liquid phase is negligible. Together with the real part, the complex viscosity of the partially solidified alloy melt therefore reflects the viscoelastic behavior while the liquid alloy viscosity has to be determined from separate measurements of samples with nominal compositions of the interdendritic liquid at any temperature in the partially solidified temperature range. With the complex viscosity mainly reflecting the solid phase of the liquid–solid two-phase mixture, the measured phase shift of more than 45° then suggests that the solid phase in the partially solidified temperature region behaves liquid-like from a rheological viewpoint. This somewhat provocative finding points towards the new insight that oscillatory measurements can achieve in the partially solidified range of alloys.

5 Conclusions

Rotational viscosity measurements with a Searle-type concentric cylinder approach demonstrate the influence of the fraction solid on the viscosity values for hypoeutectic Al-Cu alloys. A rapid increase in viscosity is observed beyond a solid fraction of 0.4–0.6, but the viscosity then decreases despite an increase in the solid fraction. Optical microscopy reveals a dendritic solidification morphology that suggests dendrite fragmentation to cause the observed viscosity decrease. A clear scaling of viscosity with solid fraction emerges from oscillatory measurements. Amplitudes of a few milli radians yield a complex viscosity that displays a steep viscosity increase between about 0.2 and 0.6 before leveling off. The phase shift between real and imaginary parts of the complex viscosity starts out at close to 90° in the liquid state and with solid fraction of less than about 0.2, but then decreases sharply

to a nearly constant value of about 0.65–0.7 at solid fractions beyond 0.2 to 0.4. Measurements of fully liquid alloys at interdendritic compositions demonstrate that the interdendritic liquid viscosity is about three orders of magnitude smaller than the measured real and imaginary parts of the partially solidified alloy. Oscillatory measurements therefore capture largely the viscoelastic behavior of the solid skeleton in the partially solidified alloy. The phase shift during oscillatory measurements with 1 mrad amplitude of about 60 to 70° suggests a rheological behavior of the solid phase that resembles a liquid rather than a solid material. The current work points toward new ways to determine the constitutive behavior of partially solidified alloys over a broad range of solid fraction, which would support simulations of manufacturing processes such as casting, welding, or additive manufacturing.

Acknowledgements The authors thank the Air Force Research Laboratory, Materials and Manufacturing Directorate (AFRL/RXMS) for support via contract FA8650-18-C-5700.

Author's contribution Material preparation, data collection and analysis were performed by Lakshmi Ravi Narayan. The first draft of the manuscript was written by Lakshmi Ravi Narayan and Rainer J. Hebert, and all authors commented on previous versions of the manuscript. All authors read and approved the final manuscript.

Funding The authors have no relevant financial or non-financial interests to disclose.

Data availability The datasets generated during and/or analyzed during the current study are available from the corresponding author on request.

Declarations

Conflict of interest The authors have no conflicts of interest to declare that are relevant to the content of this article.

Open Access This article is licensed under a Creative Commons Attribution 4.0 International License, which permits use, sharing, adaptation, distribution and reproduction in any medium or format, as long as you give appropriate credit to the original author(s) and the source, provide a link to the Creative Commons licence, and indicate if changes were made. The images or other third party material in this article are included in the article's Creative Commons licence, unless indicated otherwise in a credit line to the material. If material is not included in the article's Creative Commons licence and your intended use is not permitted by statutory regulation or exceeds the permitted use, you will need to obtain permission directly from the copyright holder. To view a copy of this licence, visit <http://creativecommons.org/licenses/by/4.0/>.

References

1. Flemings MC (1974) Solidification Processing. McGraw-Hill Inc, UK

2. Flemings MC (1991) Behavior of metal alloys in the semi solid state. *Metall Trans A* 22B:269–293. <https://doi.org/10.1007/BF02651227>
3. Gomez IV, Viteri EV, Montero J, Djurdjevic M, Huber G (2018) The determination of dendrite coherency point characteristics using three new methods for aluminum alloys. *Appl Sci* 8:1236. <https://doi.org/10.3390/app8081236>
4. Eskin DG, Katgerman L (2007) A quest for a new hot tearing criterion. *Metall Mater Trans A* 38(7):1511–1519
5. Arnberg L, Chai G, Backerud L (1993) Determination of dendritic coherency in solidifying melts by rheological measurements. *Mater Sci Eng, A* 173:101–103
6. Sumitomo T, StJohn DH, Steinberg T (2000) The shear behaviour of partially solidified Al–Si–Cu alloys. *Mater Sci Eng A* 289:18–29. [https://doi.org/10.1016/S0921-5093\(00\)00936-9](https://doi.org/10.1016/S0921-5093(00)00936-9)
7. Dahle AK, Arnberg L (1996) The rheological properties of solidifying aluminum foundry alloys. *JOM* 48:34–37
8. Dahle AK, Tondel PA, Paradies CJ, Arnberg L (1996) Effect of grain refinement on the fluidity of two commercial Al–Si foundry alloys. *Metall Mater Trans A* 27A:2305–2313. <https://doi.org/10.1007/BF02651885>
9. Das P, Samanta SK, Chattopadhyay H, Dutta P, Barman N (2013) Rheological characterization of semi-solid a356 aluminium alloy. *Solid State Phenom* 192–193:229–234. <https://doi.org/10.4028/www.scientific.net/SSP.192-193.329>
10. Eskin DG, Suyitno KL (2004) Mechanical properties in the semi-solid state and hot tearing of aluminium alloys. *Prog Mater Sci* 49:629–711. [https://doi.org/10.1016/S0079-6425\(03\)00037-9](https://doi.org/10.1016/S0079-6425(03)00037-9)
11. Braccini M, Martin CL, Tourabi A, Brechet Y, Suery M (2002) Low shear rate behavior at high solid fractions of partially solidified Al–8 wt.% Cu alloys. *Mater Sci Eng A* 337:1–11. [https://doi.org/10.1016/S0921-5093\(02\)00042-4](https://doi.org/10.1016/S0921-5093(02)00042-4)
12. Ferrante M, de Freitas E (1999) Rheology and microstructural development of a Al–4wt% Cu alloy in the semi-solid state. *Mater Sci Eng A* 271:172–180. [https://doi.org/10.1016/S0921-5093\(99\)00226-9](https://doi.org/10.1016/S0921-5093(99)00226-9)
13. Tocci M, Pola A, Modigell M (2019) Rheological investigation of semisolid AlSi7 alloy by means of oscillation experiments. *Solid State Phenom* 285:385–390. <https://doi.org/10.4028/www.scientific.net/SSP.285.385>
14. Ganesan S, Speiser R, Poirier DR (1987) Viscosities of aluminum-rich Al–Cu liquid alloys. *Metall Trans B* 18B:421–424. <https://doi.org/10.1007/BF02656162>
15. Fang Y, Galenko PK, Liu D, Hack K, Rettenmayr M, Lippmann S (2022) Thermodynamic description of metastable fcc/liquid phase equilibria and solidification kinetics in Al–Cu alloys. *Phil Trans Royal Soc A* 380:20200327. <https://doi.org/10.1098/rsta.2020.0327>
16. Hu Z, Nie X, Qi Y, Zhang H, Zhu H (2021) Cracking criterion for high strength Al–Cu alloys fabricated by selective laser melting. *Additive Manufact* 37:101709. <https://doi.org/10.1016/j.addma.2020.101709>
17. Yang Z, Fang H, Jin K, He J, Ge W, Yan W (2022) Modeling of microstructure evolution coupled with molten pool oscillation during electron beam welding of an Al–Cu alloy. *Int J Heat Mass Transfer* 189:122735
18. Du M, Wang F, Du X, Wang W, Mao P, Wang Z, Zhou L, Liu Z (2022) Effects of Alternating Magnetic Field on the Hot Tearing Susceptibility and Microstructure of Al–5Cu Alloy. *Int J Metalcast*. <https://doi.org/10.1007/s40962-022-00781-1>
19. Searle GFC (1912) A simple viscometer for very viscous liquids. *Proc Camb Philos Soc* 16:600–606
20. Mezger TG (2014) *The rheology handbook*. Vincentz Network, UK
21. Malik MM, Jeyakumar M, Hamed MS, Walker MJ, Shankar S (2010) Rotational rheometry of liquid metal systems: Measurement geometry selection and flow curve analysis. *J Nonnewton Fluid Mech* 165:733–742. <https://doi.org/10.1016/j.jnnfm.2010.03.009>
22. Modigell M, Harboe S, Pola A, Zang C (2015) Semisolid metals: a suspension with Non-Newtonian Liquid Matrix. *Solid State Phenomena* 217:166–173
23. Slezak M (2018) Study of semi-solid magnesium alloys (with RE elements) as a non-Newtonian fluid described by rheological models. *Metals* 8(8):222. <https://doi.org/10.3390/met8040222>
24. Ma Z, Zhang H, Zhang X et al (2019) *J Alloy Compd* 803:1141–1154. <https://doi.org/10.1016/j.jallcom.2019.06.345>
25. Atkinson HV (2005) Modelling the semisolid processing of metallic alloys. *Prog Mater Sci* 50:341–412. <https://doi.org/10.1016/j.pmatsci.2004.04.003>
26. Zhu BW, Li LX, Liu X, Zhang LQ, Xu R (2015) Effect of viscosity measurement method to simulate high pressure die casting of thin-wall AlSi10MnMg alloy castings. *J Mater Eng Perform* 24:5032–5036. <https://doi.org/10.1007/s11665-015-1783-8>
27. Hu XG, Zhu Q, Atkinson HV et al (2017) A time-dependent power law viscosity model and its application in modelling semi-solid die casting of 319s alloy. *Acta Mater* 124:410–420. <https://doi.org/10.1016/j.actamat.2016.11.031>
28. Deschamps J, Georgelin M, Pocheau A (2008) Growth directions of microstructures in directional solidification of crystalline materials. *Phys Rev E* 78:011605
29. Schlichting H, Gersten K (2017) *Unsteady turbulent boundary layers*. In: *Boundary-layer theory*. Springer, Berlin, pp 645–651
30. Schramm G (2000) *A practical approach to rheology and rheometry*. Thermo Haake Rheology, Karlsruhe, Germany
31. Jones WRD, Bartlett WL (1952) The viscosity of aluminium and binary aluminium alloys. *J Inst Met* 81:145–152

Publisher's Note Springer Nature remains neutral with regard to jurisdictional claims in published maps and institutional affiliations.